Available online at www.sciencedirect.com
ScienceDirect
Biologicals 36 (2008) 27–36
IABS BIOLOGICALS
www.elsevier.com/locate/biologicals

Prion removal by nanofiltration under different experimental conditions

Mikihiro Yunoki [a,b,*], Hiroyuki Tanaka [b], Takeru Urayama [a,b], Shinji Hattori [b], Masahiro Ohtani [b], Yuji Ohkubo [b], Yoshiyasu Kawabata [b], Yuuki Miyatake [b], Ayako Nanjo [b], Eiji Iwao [c], Masanori Morita [b], Elaine Wilson [d], Christine MacLean [d], Kazuyoshi Ikuta [a]

[a] *Department of Virology, Research Institute for Microbial Diseases, Osaka University, Japan*
[b] *Research & Development Division, Benesis Corporation, Japan*
[c] *Pharmaceutical Research Division, Mitsubishi Pharma Corporation, Japan*
[d] *BioReliance, Invitrogen BioServices, UK*

Received 21 December 2006; revised 11 April 2007; accepted 27 April 2007

Abstract

Manufacturing processes used in the production of biopharmaceutical or biological products should be evaluated for their ability to remove potential contaminants, including TSE agents. In the present study, we have evaluated scrapie prion protein (PrP^{Sc}) removal in the presence of different starting materials, using virus removal filters of different pore sizes. Following 75 nm filtration, PrP^{Sc} was detected in the filtrate by Western blot (WB) analysis when a "super-sonicated" microsomal fraction derived from hamster adapted scrapie strain 263K (263K MF) was used as the spike material. In contrast, no PrP^{Sc} was detected when an untreated 263K MF was used. By using spike materials prepared in a manner designed to optimize the particle size distribution within the preparation, only 15 nm filtration was shown to remove PrP^{Sc} to below the limits of detection of the WB assays used under all the experimental conditions. However, infectious PrP^{Sc} was recovered following 15 nm filtration under one experimental condition. The results obtained suggest that the nature of the spike preparation is an important factor in evaluating the ability of filters to remove prions, and that procedures designed to minimize the particle size distribution of the prion spike, such as the "super-sonication" or detergent treatments described herein, should be used for the preparation of the spike materials.

Keywords: Prion; Removal; Filter; Clearance study; Spike material

1. Introduction

The transmission of variant Creutzfeldt–Jakob disease (vCJD) through blood transfusion has been of increasing concern, since a fourth possible transmission case was reported [1]. In addition, prions have been detected in the buffy coat separated from the blood of hamsters infected with scrapie, using a biochemical assay (protein misfolding cyclic amplification, or PMCA) [2]. Infectious prions are thought to be the causative agent of the transmissible spongiform encephalopathy (TSE) diseases, which include Creutzfeldt–Jakob disease (CJD), vCJD, and bovine spongiform encephalopathy (BSE). Therefore, to reduce the risk of transmission when raw materials for protein products (such as plasma) are contaminated with infectious prions, measures should be introduced to decrease the prion load, to evaluate the risk to the product, and to introduce prion removal/inactivation step(s) in the manufacturing process, if feasible [3–5]. Unlike viruses, the minimum infectious prion unit does not exist as a single particle. The infectious prion unit is believed to be composed of protein polymers/aggregates, rather than a prion particle. The unusual nature of the prion agent makes it particularly important to

* Corresponding author. Hirakata Research Laboratory, Research & Development Division, Benesis Corporation, 2-25-1 Shodai-Ohtani, Hirakata, Osaka 573-1153, Japan. Tel.: +81 72 850 0100; fax: +81 72 864 2341.
E-mail address: yunoki.mikihiro@mk.m-pharma.co.jp (M. Yunoki).

1045-1056/07/$34.00
doi:10.1016/j.biologicals.2007.04.005

consider the effect of the prion spike material when evaluating process steps for prion clearance. A rationale for the choice of the spike preparation used for such evaluation studies should be provided [4].

Several prion strains have been used to evaluate manufacturing processes for their ability to remove TSE agents, including hamster scrapie prion protein (PrP^{Sc}, 263K or Sc237), and mouse PrP^{BSE} (301V). In a polyethylene glycol (PEG) fractionation process, hamster PrP^{Sc} and human PrP^{vCJD}, prepared using the same methodology, were reported to behave in a very similar manner [6]. Different prion spike preparations have been used to investigate prion removal, including crude brain homogenate (BH), microsomal fraction (MF), caveolae-like domains (CLDs), and purified PrP^{Sc}. Of these materials, purified PrP^{Sc} was reported to behave differently from the other preparations in an 8% ethanol fractionation step [7]. This result suggests that the methods used to prepare the prion spike material may be a critical factor in prion clearance studies. Furthermore, these reports are useful in providing a rationale for the choice of the prion source and spike preparation used for such evaluation studies [8].

Tateishi et al. reported that sarkosyl influenced the ability of BMM40 filters to remove prions, using BH derived from CJD-infected mice [9]. The presence of sarkosyl was also shown to significantly reduce the capacity of Planova (P)-35N to remove the scrapie agent ME7, while filtration with P-15N resulted in the complete removal of infectivity, to below the limit of detection of the bioassay used, in both the presence and absence of sarkosyl [10]. Van Holten et al. evaluated the capacity of Viresolve 180 membranes (designed for virus removal from proteins of <180 kDa) to remove prions by using BH which was lysolecithin-treated, sonicated, and subsequently passed through a 100 nm filter (SBH), and demonstrated removal of PrP^{Sc} down to the limit of detection of the Western blot assay used. They argued that by using a better defined spike material, where the size of the scrapie particles was limited, the results may be more relevant with respect to the removal of potential TSE infectivity in plasma than previous studies that used a less well-defined BH [11].

Aggregation of the prion protein is a critical parameter when evaluating nanofiltration steps. The actual form of the infectious agent present in plasma in natural infection is not known. In addition, nanofiltration is typically performed late in the downstream processing, after protein purification steps, which may result in removal of larger or aggregated prion forms. Therefore, use of a spike preparation containing large aggregates may result in an over-estimate of the prion removal capacity of a filter. Although the reports described above, and others, have shown excellent prion removal ability for a number of filters, most reports have not described the particle size distribution of the prion protein in the spike preparations used. Therefore, in this study we have investigated the prion removal capacity of P-35N, P-20N and P-15N filters under diverse conditions, considering the particle size distribution of the MF preparations used.

2. Materials and methods

2.1. Preparation of microsomal fraction (MF)

Brains removed from hamsters infected with scrapie strain 263K [12] (originally obtained from the Institute for Animal Health, Edinburgh, UK), were homogenized in phosphate buffered saline (PBS) until homogeneous, to a final concentration of 10% (w/v). The homogenate was clarified by low speed centrifugation, to remove larger cell debris and nuclei, and the supernatant material was then further clarified by centrifugation at 8,000 × *g* for 10 min at 4 °C, before being ultracentrifuged at 141,000 × *g* for 60 min at 4 °C, to concentrate the scrapie fibrils, and small membrane vesicles and fragments. The pelleted material was resuspended in PBS, aliquoted, and stored at −80 °C. This material was designated 263K MF. Prior to use, stocks were thawed at 37 °C, and sonicated 2 × 4 min on ice water (Ultrawave ultrasonic bath model #U100, 130 W 30 kHz, Ultrawave Ltd., Cardiff, UK). Six independent batches of 263K MF were used in this study. These batches are designated 263K MF preparation lots A–F (Tables 1–3). Normal MF, derived from normal (i.e. uninfected) hamster brain material, was also prepared as described above.

Since we were unable to measure the particle size distribution of contaminated materials in our facility, we used normal MF, and investigated changes in the particle size distribution following strong sonication or treatment with detergent. Various concentrations of sarkosyl (*N*-lauroylsarcosine sodium salt, Nacalai Tesque, Inc., Kyoto, Japan), lysolecithin (L-α-lysophosphatidylcholine, Sigma-Aldrich Corp., St. Louis, USA), Triton X-100 (polyethylene glycol mono-*p*-isooctylphenyl ether, Nacalai Tesque, Inc.), TNBP (tri-n-butyl phosphate, Wako Pure Chemical Industries, Ltd., Osaka, Japan), and/or 1% Tween 80 (Nacalai Tesque, Inc.) were added to normal MF. Changes in the particle size distribution were then monitored by dynamic light scattering method using volume-weighted gaussian analysis using a submicrometer particle sizer (NICOMP Type 370, Particle Sizing Systems, Inc., Santa Barbara, USA). To evaluate the effect of strong sonication, normal MF was sonicated using a closed system ultrasonic cell disruptor (Bioruptor UCD-200T, CosmoBio Co. Ltd., Tokyo, Japan) with a resonance chip set in the tube. Sonication was performed for 1 min at 20 kHz, 200 W in a cold water-bath. Ten cycles of sonication were performed, with a 1 min

Table 1
Scrapie infectivity in different 263K MF preparations[a]

	Log_{10} LD_{50}/ml	SE at 95% probability
Non-super-sonicated 263K MF lot C	5.7	0.44
Super-sonicated 263K MF lot C	6.0	0.53
Super-sonicated 263K MF lot D	5.3	0.69
SD-treated, ultracentrifuged, super-sonicated and 220 nm-filtered 263K MF lot C	6.9	0.69

[a] This bioassay study was performed in accordance with GLP regulations.

Table 2
Removal of PrP^{Sc} from PrP^{Sc}-inoculated PBS

	PVDF filter				Planova filter					
	220 nm		100 nm		P-75N (72 ± 2 nm)		P-35N (35 ± 2 nm)		P-15N (15 ± 2 nm)	
Super-sonicated	+	−	+	−	+	−	+	−	+	−
Before filtration	4.2/3.5[a]	3.5/4.2	4.2/3.5	3.5/4.2	4.2/4.2	3.5/4.2	4.2/4.2	3.5/4.2	4.2/4.2	3.5/4.2
Filtered	3.8/3.8	3.1/3.8	3.8/3.1	2.4/3.1	2.4/2.4	<1.0/<1.0	<1.0/<1.0	<1.0/<1.0	<1.0/<1.0	<1.0/<1.0
LRF[b]	0.4/−0.3	0.4/0.4	0.4/0.4	1.1/1.1	1.8/1.8	≥2.5/≥3.2	≥3.2/≥3.2	≥2.5/≥3.2	≥3.2/≥3.2	≥2.5/≥3.2

Data represents total PrP^{Sc} present in samples, expressed as $\log_{10}$ arbitrary units, following Western blot analysis as described for WB1. This study was performed in accordance with GLP regulations.

[a] Two independent batches of 263K MF were used: lot C (left) and lot D (right), respectively.

[b] LRF, log reduction factor = total PrP^{Sc} in input/total PrP^{Sc} in filtrate, expressed as a $\log_{10}$ value.

interval between each sonication treatment. During the treatment cycle, the particle size distribution was monitored. We named this treatment cycle "super-sonication".

Different preparations of 263K MF, treated with various combinations of detergent, ultracentrifugation and/or "super-sonication", were used as the spiking agent in the process evaluation studies, and are described in the relevant methods sections below.

2.2. Detection of PrP^{Sc} by Western blotting (WB)

To determine the relative levels of PrP^{Sc} present in different samples, WB assays were performed. Three slightly different WB methodologies were applied over the course of the studies, all of which are based on detection of the disease-associated, protease-resistant form of the prion protein (PrP^{Sc}), using the monoclonal antibody 3F4 (Signet Laboratories, Inc., Dedham, USA) [13]. WB methods 1 and 2 were developed independently, and use different approaches to calculate the titer of PrP^{Sc}. As these assays were performed as part of GLP studies intended for regulatory submission, the results are presented as reported in these studies.

2.2.1. Method 1 (WB1)

Samples and controls were either tested directly, or first ultracentrifuged at 141,000 × *g* for 60 min at 4 °C, and the pelleted material then resuspended in PBS. Ultracentrifugation was performed to concentrate the PrP^{Sc} present in large volume samples, and to remove soluble proteins or buffer components that might interfere with the WB assay. Samples were digested with proteinase K (Roche Diagnostics, GmbH, Penzberg, Germany) for 60 min at 37 °C. The optimal concentration of proteinase K, to remove any background that could interfere with the detection of PrP^{Sc} and to allow effective recovery of the PrP^{Sc} protein, was previously established for each sample. Digested samples were mixed 1:1 with Laemmli sample buffer (62.5 mM Tris–HCl, pH 6.8, 25% (v/v) glycerol, 2% (w/v) SDS, and 0.01% (w/v) bromophenol blue, BioRad Laboratories Inc., Hercules, USA) containing 5% (v/v) β-mercaptoethanol. After boiling, serial 5-fold dilutions of

Table 3
Removal of PrP^{Sc} from PrP^{Sc}-inoculated plasma preparations[a]

Filter	P-35N (35 ± 2 nm)		P-20N (19 ± 2 nm)		P-15N (15 ± 2 nm)			
Preparation	IVIG	Haptoglobin	IVIG	Haptoglobin	Antithrombin			Thrombin
Spike material	263K sMF[c]	263K sMF[c]	263K sMF[d]	263K dsMF[e]	263K dMF[f]	263K sMF[c]		263K dsMF[e]
MF preparation lot.	C/D	B	E/F	E/F	A/A	B		C/D
Spike ratio	1/100	1/200	1/20	1/200	1/50	1/21		1/20
Detection method[b]	WB1	WB3	WB2	WB2	WB1	WB3	BA	WB1
Before filtration	3.2/2.5	2.4	6.8/6.8	6.7/6.1	3.1/3.1	3.6	+ve	3.7/3.7
Filtered	0.8/0.8	<1.0	4.8/4.3	4.8/4.7	0.0/0.0	<0.8	+ve	<0.2/<0.2
Log reduction factor	2.4/1.7	≥1.4	2.0/2.5	1.9/1.4	≥3.1/≥3.1	≥2.8	NA	≥3.5/≥3.5

Abbreviations used: 263K MF, microsomal fraction derived from hamster adapted scrapie strain 263K; IVIG, intravenous immunoglobulin; 263K sMF, "super-sonicated" 263K MF; WB, Western blotting; 263K dsMF, detergent treated and "super-sonicated" 263K MF; 263K dMF, detergent treated 263K MF; BA, bioassay; +ve, scrapie positive.

[a] Scaled down conditions were designed according to current guidelines. However, in a study using P-35N filter and haptoglobin, clogging of the filter occurred, and the filtration was subsequently terminated.

[b] WB1, WB2, and WB3 mean Western blotting methods 1, 2 and 3, respectively. The studies involving the use of WB1 and WB2 were performed in accordance with GLP regulations; the studies involving the use of WB3 and the qualitative BA shown in this table, were performed as non-GLP studies.

[c] 263K MF was "super-sonicated" then 220 nm-filtered prior to spiking.

[d] 263K MF was ultracentrifuged at 141,000 × *g* for 60 min at 4 °C, resuspended in buffer equivalent to the starting material without protein, "super-sonicated", and 220 nm-filtered prior to spiking.

[e] 263K MF was "SD-treated", ultracentrifuged at 141,000 × *g* for 60 min at 4 °C, resuspended in the starting material (thrombin) or saline (haptoglobin), and "super-sonicated". These materials were 220 nm-filtered prior to spiking.

[f] 263K MF was treated with 0.1% sarkosyl for 30 min at room temperature.

the sample were then prepared and subjected to electrophoresis using 12% (w/v) SDS-polyacrylamide gels. Proteins were transferred from the gels to 0.45 μm PVDF membranes (Immobilon-P, Millipore Corp., Billerica, USA), and non-specific binding sites on the membranes were then blocked by overnight incubation in buffer containing dried milk and Tween 20. The blocked membranes were incubated with monoclonal antibody 3F4, washed extensively, and then incubated with a secondary horseradish peroxidase (HRP)-conjugated anti-mouse antibody (Sigma-Aldrich Corp.). After further extensive washing, bound antibody was detected using an ECL-Plus detection system (GE Healthcare UK Ltd, Buckinghamshire, UK) and exposure to blue-light sensitive film.

The level of PrP^{Sc} present in each sample was calculated based on the end-point dilution after analysis by WB. The end-point dilution for each titration was taken as the first dilution at which the 28 kDa PrP^{Sc} protein could not be detected. The reciprocal of this dilution was then taken as the titer of the agent, and expressed in arbitrary units/ml.

2.2.2. Method 2 (WB2)

WB was performed essentially as described by Lee et al. [14]. Briefly, samples were digested with proteinase K at approximately 6 U/ml for 60 min at 37 °C and centrifuged at approximately 20,000 × *g* for 60 min at 4 °C. The pellet was then resuspended and denatured in a 1:1 mix of supernatant and sample buffer (62.5 mM Tris–HCl, pH 6.8, 10% (v/v) glycerol, 2% (w/v) SDS and 0.0025% (w/v) bromophenol blue, Invitrogen Corp. Carlsbad, USA), by heating at approximately 100 °C. Serial 3.2-fold (0.5 $\log_{10}$) dilutions of the sample were prepared, and loaded onto 12% (w/v) SDS-polyacrylamide gels. Following electrophoresis, proteins were transferred to nitrocellulose membranes (Invitrogen Corp.), and the membranes blocked using buffer containing dried milk and Tween 20 for 1–2 h at room temperature. The blocked membranes were then incubated with monoclonal antibody 3F4, washed extensively, and incubated with a secondary alkaline phosphatase (AP)-conjugated anti-mouse antibody (Cambridge Biosciences Ltd., Cambridge, UK). After further extensive washing, bound antibody was detected using a CDP Star/Nitroblock II detection system (Applied Biosciences, Bedford, USA) and exposure to blue-light sensitive film.

The titer of PrP^{Sc} present in each sample was calculated slightly differently from WB1 and WB3. The end-point dilution for each titration was taken as the last dilution at which the 28 kDa PrP^{Sc} protein could be detected. The reciprocal of this dilution was then taken as the amount of agent in the sample volume tested, and was adjusted for the volume tested and any concentration factors, to give a titer/ml for the original process sample.

2.2.3. Method 3 (WB3)

Samples were ultracentrifuged twice at 150,000 × *g* for 1 h. The samples in the precipitates were then resuspended in PBS at 1/1 or 1/10th volume of the original. Resuspended samples were treated with proteinase K at a final concentration of 10–100 μg/ml. After incubation at 37 °C for 60 min, samples were treated with 10 mM 4-(2-aminoethyl)-benzene sulfonyl fluoride hydrochloride (AEBSF) at room temperature for 10 min, then mixed with 5× SDS-polyacrylamide gel electrophoresis (PAGE) sample buffer (300 mM Tris–HCl, 12% (w/v) SDS, 25% (v/v) glycerol, and 0.025% (w/v) bromophenol blue, pH 6.8, with 25% (v/v) β-mercaptoethanol) and heated at 100 °C for 5 min. Samples were serially 5-fold diluted with 1× PAGE dilution buffer (60 mM Tris–HCl, 2.4% (w/v) SDS, 5% (v/v) glycerol, and 0.005% (w/v) bromophenol blue, pH 6.8). SDS-PAGE was performed at 30 mA per gel for approximately 42 min. The proteins in the gel were transferred to 0.45 μm PVDF membranes. After treating with blocking buffer (5.0% (w/v) skimmed milk in PBS, 0.05% (v/v) Tween 20), the membrane was incubated with monoclonal antibody 3F4 at 4 °C overnight, then incubated with HRP-conjugated sheep anti-mouse IgG (Sigma-Aldrich Corp.). Bound antibody was visualized by chemiluminescence (ECL-Plus) on X-ray film. The titer of PrP^{Sc} present in the samples was calculated as described for method 1 in Section 2.2.1.

2.3. Evaluation of PrP^{Sc} removal by filtration

A 10% (v/v) concentration of "super-sonicated" 263K MF was prepared in PBS, and 10 ml aliquots were then filtered through a 220 nm or a 100 nm 4 cm^2 PVDF filter (Millex-GV or -VV, Millipore Corp.). In addition, 25 ml aliquots of "super-sonicated" 263K MF in PBS were filtered through a 0.01 m^2 P-75N (72 ± 2 nm), P-35N (35 ± 2 nm), or P-15N (15 ± 2 nm) filter (Asahi Kasei Medical Co., Ltd. Tokyo, Japan). Two independent batches of 263K MF were used. WB1 analysis of samples before and after filtration was performed to determine the removal of PrP^{Sc} under the different conditions. Non-sonicated 263K MF (from the same batch of 263K MF) was also filtered as a control.

2.4. Hamster bioassay to determine the infectious titer of 263K scrapie stocks

Three- to four-week-old female specific pathogen-free (SPF) Syrian hamsters were used in these experiments. Serial 10-fold dilutions of each sample or positive control were prepared in PBS. Six hamsters per sample dilution were inoculated intra-cerebrally with 0.02 ml per animal. The inoculated animals were monitored daily for general health, and weekly for clinical evidence of scrapie. Animals were euthanized once advanced signs of scrapie were evident, or at the end of the assay period (200 days). The brain was removed from each hamster following euthanasia: one half was fixed for histopathology and the other half was stored frozen at −70 °C for further analysis if required. For histopathological analysis, sections taken at four standard coronal levels, to cover the nine areas of the brain which are recognized to be mostly infected by the scrapie agent, were stained with hematoxylin and eosin, and scored for the presence or absence of scrapie lesions [15]. Histopathological analysis was performed on samples from around the clinical end-point of the titration assays, to confirm the clinical results. Hamsters that died during the

course of the study for reasons other than scrapie infection were not included in the final calculation of infectious titers. Infectious titers were expressed as a 50% lethal dose (LD_{50}) according to the method of Kärber [16].

Samples taken before and after filtration during the P-15N/antithrombin (AT; previously named antithrombin-III) study were tested for the presence of scrapie infectivity using a qualitative hamster bioassay. Syrian hamsters were inoculated with undiluted samples only, as described above, except that only three animals were used per sample.

2.5. Evaluation of PrP^{Sc} removal in the presence of plasma preparations

To investigate whether differences in how the scrapie spike material was prepared influenced our evaluation of prion removal, two different spiked preparations were compared using the manufacturing process for preparing AT (Neuart®, Benesis Corp., Osaka, Japan). Samples taken during the actual manufacturing process, immediately before the Planova step, were spiked with 263K MF treated with 0.1% (w/v) sarkosyl for 30 min at room temperature, or with 220 nm-filtered "super-sonicated" 263K MF. The spiked AT materials were then passed through a P-15N filter. The influence of different filtration conditions on the removal of PrP^{Sc} was compared for the same spike preparations, and for different spike preparations, using heat/PEG-treated intravenous immunoglobulin (IVIG) (Venoglobulin-IH, Benesis Corp.) and haptoglobin (Haptoglobin Injection-Yoshitomi, Benesis Corp.). Samples taken during the actual manufacturing process, immediately before the Planova step, were spiked with: 220 nm-filtered "super-sonicated" 263K MF (IVIG/P-35N and haptoglobin/P-35N); 263K MF ultracentrifuged at 141,000 × *g* for 60 min at 4 °C, resuspended in buffer equivalent to the starting material without protein, "super-sonicated" and 220 nm-filtered (IVIG/P-20N); or 263K MF treated with 0.3% (v/v) TNBP/1% (v/v) Tween 80 for 6 h at 30 °C ("SD treatment"), ultracentrifuged at 141,000 × *g* for 60 min at 4 °C, resuspended in saline, "super-sonicated", and 220 nm-filtered (haptoglobin/P-20N). The spiked material was then passed through either a P-35N filter or a P-20N filter (19 ± 2 nm). Although not part of the manufacturing process for haptoglobin, the SD treatment was included for the spiked preparation in an effort to reduce the clogging of the filter that occurs following the addition of a prion spike. Filtration processes for the thrombin preparation (Thrombin-Yoshitomi, Benesis Corp.) were also investigated. For thrombin, a sample taken during the actual manufacturing process immediately before the Planova step was spiked with 263K MF subjected to "SD treatment" followed by ultracentrifugation at 141,000 × *g* for 60 min at 4 °C, resuspended in the starting material, "super-sonicated" and 220 nm-filtered, and the spiked material then passed through a P-15N filter.

The experimental conditions used in the prion removal studies were designed to mimic the conditions used during the actual manufacturing process for the relevant product. For all processes, samples were analyzed by WB. The $\log_{10}$ reduction factor (LRF) for PrP^{Sc} was calculated for each filtration run, by comparing the total amount of PrP^{Sc} present in samples before and after filtration. All studies involving the use of WB1 and 2, and the quantitative bioassays, were performed in facilities in compliance with current GLP regulations. Studies involving the determination of average particle size in normal MF preparations, the use of WB3, and the qualitative bioassay, were performed as non-GLP studies.

3. Results

3.1. Influence of MF preparation method on particle size distribution

Ideally, to represent a "worst case" challenge for a filter, the smallest form of prion protein, or infectious agent, should be used. Studies to investigate the optimum method for preparing the prion spike material were therefore performed. In these studies, changes in the average particle size in normal MF were investigated, as 263K-infected brain material could not be handled within our facility. Although prion particles in MF derived from 263K-infected brain material were not investigated directly, we tried to optimize the design of our experiments by minimizing the size of particles in normal MF, as particle size may influence filtration performance (both with respect to filter blockage, and removal of PrP^{Sc}). The results are shown in Figs. 1 and 2.

Treatment of normal MF with sarkosyl or lysolecithin reduced the average size of particles to approximately 100 nm, when 0.1% or higher concentrations of the detergents were used. However, below that concentration, the particle size did not change significantly, with the exception of 0.01% lysolecithin which reduced the average particle size to approximately 300 nm (Fig. 1A,B). Treatment with Triton X-100 did not result in a significant change in particle size, even at 1% (Fig. 1C). Treatment with 0.3% TNBP or 1% Tween 80 alone was not able to reduce the particle size below 200 nm. However, when combined, one of the conditions generally used for viral inactivation ("SD treatment"), 0.3% TNBP and 1% Tween 80 reduced the average particle size to below 200 nm (Fig. 1D). These results suggest that the reduction in average particle size in normal MF depends on the choice of detergent(s), and the concentration and combination of detergent(s) used.

We also studied the effect of "super-sonication" on the particle size in normal MF. The results showed that "super-sonication" could reduce the average particle size to a very fine level in a short time, without the need to change the composition of the normal MF material (Fig. 2A). Since "super-sonication" is a temporary physical procedure, reversal of the particle size reduction may possibly occur. To exclude this possibility during the experiments, we conducted a stability study on the particle size in normal MF after "super-sonication". There was no significant change in the particle size up to 24 h after "super-sonication", with the size remaining at approximately 100 nm (Fig. 2B).

The results showed that the particle size of normal MF preparations could be reduced significantly by treatment

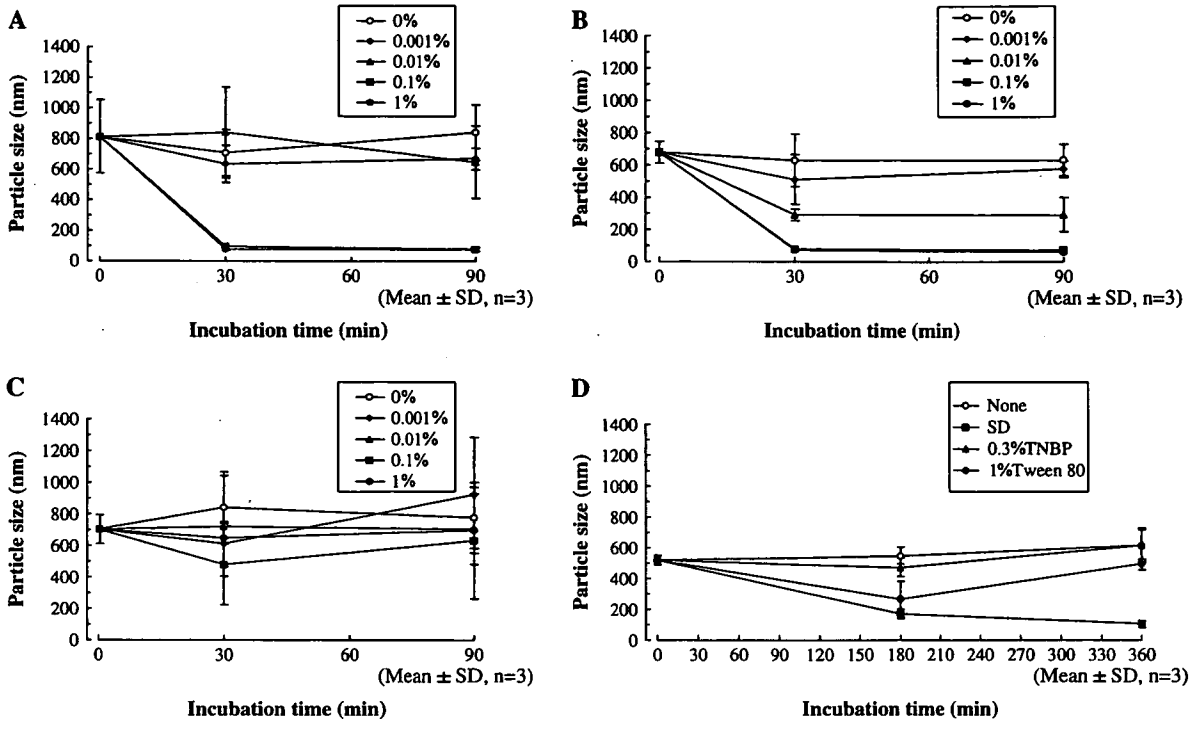

Fig. 1. Change of particle size in normal MF following treatment with various detergents. To normal MF, sarkosyl (A), lysolecithin (B), or Triton X-100 (C) was added to a final concentration of 1%, 0.1%, 0.01%, and 0.001%, respectively. The change in the average particle size was then monitored at room temperature for 90 min. In addition, TNBP or Tween 80 was added to normal MF to a final concentration of 0.3% and 1%, respectively, either alone, or in combination ("SD treatment"). The change in the average particle size was then monitored at 37 °C for 6 h (D).

with 0.1% sarkosyl, 0.1% lysolecithin, "SD treatment", or "super-sonication". The use of detergent or "SD treatment", in combination with "super-sonication", was also shown to effectively reduce the average particle size in normal MF preparations, to comparable levels to the individual treatments alone (data not shown). "Super-sonication" has an advantage over the other treatments in that it can minimize the change of composition of samples taken from the manufacturing process, as it does not require the addition of reagent(s) to the normal MF. For this reason, "super-sonication" is considered to be a useful approach for the treatment of 263K MF for process evaluation. "SD treatment", although slightly less effective, is used in many manufacturing processes, and may therefore be useful alone, or in combination with "super-sonication", for the process evaluation of products whose manufacturing process includes an "SD treatment" step. These approaches, alone or in combination, may also be useful to prevent the clogging of filters that can occur during spiking studies.

3.2. Infectivity of PrP^{Sc} in 263K MF and influence of 263K MF preparation methods on infectivity

The effect of "super-sonication" and "SD treatment" on the infectivity of 263K MF was studied. Infectious titers of

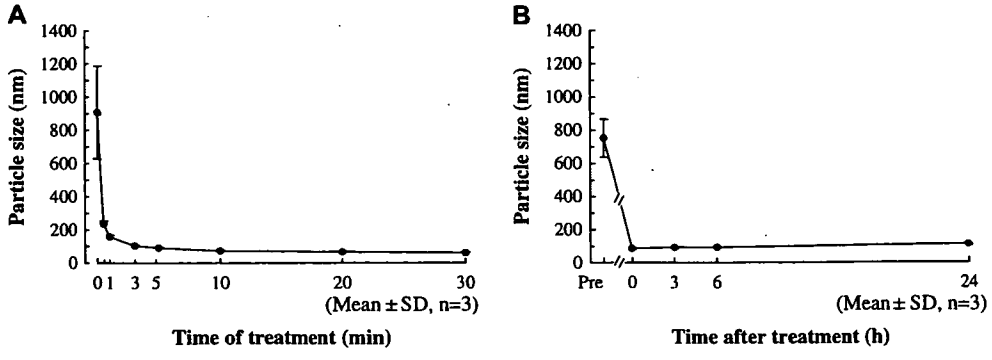

Fig. 2. Change of particle size in normal MF following intense sonication ("super-sonication"). Normal MF in a test tube equipped with a resonance chip (20 kHz, 200 W) was sonicated for 1 min in an ice bath. After 1 min, the sonication step was repeated. The change in average particle size was monitored during 30 cycles of sonication (A). After 10 cycles of sonication ("super-sonication"), normal MF was held at room temperature for 24 h, and the change in particle size was monitored (B).

263K MF, "super-sonicated" 263K MF, and 263K MF subjected to "SD treatment", ultracentrifuged at 141,000 × *g* for 60 min at 4 °C, resuspended with thrombin starting material, "super-sonicated", and 220 nm-filtered, were determined using a hamster bioassay. The results are summarized in Table 1.

The titers of two independent batches of 263K MF treated by "super-sonication" were 6.0 and 5.3 $\log_{10}$ LD_{50}/ml, respectively. The titer of the "non-super-sonicated"263K MF used to generate one of these stocks was 5.7 $\log_{10}$ LD_{50}/ml. These results suggest that "super-sonication" does not influence the infectivity of 263K MF. The titer of the 263K MF subjected to "SD treatment", ultracentrifuged at 141,000 × *g* for 60 min at 4 °C, resuspended with the thrombin starting material, "super-sonicated", and 220 nm-filtered, was 6.9 $\log_{10}$ LD_{50}/ml, which was approximately 1 log higher than that of the corresponding stock treated by "super-sonication" alone. Whether this difference is significant is unclear. The process to generate the "SD-treated" spike materials included an ultracentrifugation step. We were therefore concerned about recovery of infectivity following centrifugation, as the particle size of 263K MF was highly reduced by the "SD treatment" step. However, these results suggested that the recovery of infectious particles following ultracentrifugation was satisfactory.

Although it is possible that use of a 200 day bioassay may under-estimate the infectious titer of the 263K MF stocks, the use of a relatively short duration bioassay is considered unlikely to affect the main conclusions drawn. At least the last two dilution groups tested showed no animals with evidence of scrapie infection in all four titrations, and only three animals in the study (one in each of three separate titrations) developed clinical symptoms necessitating euthanasia later than day 131 (euthanized on days 160, 183 and 183, respectively), suggesting the titers obtained for all the stocks are close to end-point (data not shown). In addition, as others have demonstrated that treatment with detergent, and exposure to treatments that result in inactivation of the scrapie agent, such as heat or NaOH, may result in extended incubation periods for clinical scrapie, if anything the results may under-estimate the relative titers of the treated stocks [17,18]. Therefore, the bioassay results support the conclusion that "super-sonication" of 263K MF stocks, with or without "SD treatment", does not appear to significantly reduce the infectious titer of the stock, and that these preparations are therefore suitable for use in prion clearance studies.

3.3. Removal of PrP^{Sc} by various filters

To determine whether "super-sonication" influenced the $\log_{10}$ reduction observed for PrP^{Sc} following filtration under defined conditions, "super-sonicated" or "non-super-sonicated" stocks of 263K MF were diluted in PBS, and then filtered through 220 nm, 100 nm, P-75N, P-35N and P-15N filters. Samples were analyzed by WB. The results are summarized in Table 2. The use of "super-sonicated" 263K MF appeared to result in lower $\log_{10}$ reduction values, supporting the idea that "super-sonication" of 263K MF produces a more severe challenge for a filter step. An approximately 5-fold higher $\log_{10}$ reduction factor was observed for "non-super-sonicated" stocks, for the 100 nm and P-75N filters, for both stocks tested. No significant loss of PrP^{Sc} was observed with either spiking material with 220 nm filtration, and no PrP^{Sc} was detected in the filtrates following P-35N and P-15N filtration.

Previously, we have observed some removal of PrP^{Sc} in some lots of "non-super-sonicated" 263K MF by 220 nm filtration. Strict control of the methodology used to generate the 263K MF stocks appeared to prevent this, suggesting that the method of preparing the 263K MF itself may influence the particle size distribution (data not shown).

3.4. Removal of PrP^{Sc} by Planova filters in the presence of plasma preparations

Removal of PrP^{Sc} by P-15N, P-20N, and P-35N filters was evaluated in the presence of a number of different plasma preparations, under conditions designed to mimic the relevant manufacturing process. The design of the experiments was similar to that of virus clearance studies. Samples were analyzed by WB, and the $\log_{10}$ reduction factor (LRF) was calculated for each filter step. The results are shown in Table 3.

Under all the experimental conditions tested, PrP^{Sc} was not detected by WB after filtration through P-15N. The LRF values were $\geq$2.8. In contrast, PrP^{Sc} was detected by WB in samples following filtration through P-20N and P-35N filters, in three out of the four processes tested, giving LRF values in the order of 2 logs. In one study, P-35N/haptoglobin, using "super-sonicated" 263K MF, PrP^{Sc} was not detected in the filtrate. However, the sensitivity of this study was low, giving a LRF of $\geq$1.4, and therefore the robustness of this filtration process was not evaluated. In the initial studies (Table 2), PrP^{Sc} was not detected in the fractions after P-35N filtration of either "super-sonicated" or "non-super-sonicated" 263K MF in PBS, resulting in log reduction factors in the order of 3 logs. The variance in the results obtained for these filters could be due to a combination of factors, including how the scrapie spike material was prepared, the composition of the starting material, and the precise filtration conditions used.

3.5. Removal of prion infectivity by Planova filters in the presence of plasma preparations

P-15N filtration was shown in these studies to be able to remove PrP^{Sc} to levels below the detection limit of the WB assays used, regardless of the method used to prepare the spike material, the composition of the start material, or the filtration conditions. However, a bioassay study for samples generated in a P-15N/AT study using 220 nm-filtered "super-sonicated" 263K MF, demonstrated that infectivity was recovered following filtration, as clinical signs appeared in all hamsters inoculated with the filtrate, and analysis of hamster brain material confirmed the clinical results. PrP^{Sc} was detected in the brain homogenates from all clinically positive hamsters by WB, and scrapie-associated lesions were observed in all the

Table 4
Scrapie infectivity in samples generated during the P-15N/AT study

	Before filtration			Filtrate		
	Animal number			Animal number		
	1	2	3	1	2	3
Appearance of clinical signs (day euthanized)	87	87	87	94	143	105
PrP^{Sc} in brain by WB3	Detected	Detected	Detected	Detected	Detected	Detected
Lesions by histopathology	+ve	+ve	+ve	+ve	+ve	+ve
Medulla (oblongata)	D,V,P	D,V,P	D,V,P	D,V,P	D,V,P	D,V,P
Cerebellum (cortex)	D	D,V,P	D,V,P	D,V,P	D,V,P	D,V,P
Midbrain	D,P	D,V,P	V,P	D,P	D,P	D,V,P
Hypothalamus	D,P	D,V,P	D,P	D,V,P	D,P	D,P
Thalamus	D,P	D,V,P	D,P	D,P	D,P	D,P
Hippocampus	NR	D,V	D	D	D,V,P	D,V
Paraterminal body	D,P	D,P	D,P	NR	D,V,P	P
Cerebral cortex (posterior midline)	D,P	D,P	D,P	D,P	D,V,P	D,V,P
Cerebral cortex (anterior midline)	D,P	D,V,P	D,V,P	D,V,P	D,V,P	D,V,P

Abbreviations used: +ve, scrapie positive; NR, no remarkable change; D, degeneration of nerve cell; V, vacuolation; P, proliferation of glial cell.

corresponding hamster brain material on histopathological observation (Table 4). Typical nerve lesions are shown in Fig. 3. Thus, P-15N filtration did not result in the complete removal of infectivity, for this process step.

4. Discussion

In this study, we have investigated the capacity of P-35N, P-20N and P-15N filters to remove the 263K scrapie prion protein, PrP^{Sc}, under the conditions used for the manufacture of four different plasma-derived products, using spike preparations designed to present a serious challenge to the filters.

Validation studies to evaluate the capacity of manufacturing processes to remove potential contaminants, including prions, are required for biological or biopharmaceutical products intended for human use. When designing these studies, a worst-case challenge should be used wherever possible, to minimize the risk of over-estimating the capacity of the process to remove such contaminants. Virus removal filters (or nanofilters) are designed to remove contaminants predominantly on the basis of size. The worst-case challenge for such steps should therefore be a preparation containing the smallest possible form of the infectious agent.

TSE clearance studies provide a particular challenge in that the nature of the infectious agent is still uncertain, and the forms of infectious agent present in plasma, and/or during the different stages of a manufacturing process, are not clearly understood. The causative agent of TSE diseases is believed to be strongly associated with, if not solely composed of, the disease-associated prion protein, PrP^{Sc}. Normal cellular PrP is a membrane-bound glycoprotein, which associates with membranes through a glycosylphosphatidylinositol (GPI) anchor. Prion infectivity is associated with heterogeneous particles, including membranes, liposomes and protein aggregates, so called prion rods. Therefore, methods which result in solubilization of membrane proteins, or dispersal of membrane fragments, vesicles and/or protein aggregates, may be expected to reduce the size of particles associated with prion infectivity.

Treatment of MF preparations derived from brains of uninfected (normal) hamsters with either detergent (0.1% lysolecithin or 0.1% sarkosyl) or extensive sonication ("super-sonication") resulted in a rapid reduction in the average particle size, to approximately 100 nm. SD treatment (1% Tween 80 and 0.3% TNBP for 6 h) also resulted in a reduction in particle size, although this was slower and less effective, reducing the average particle size to the order of 200 nm.

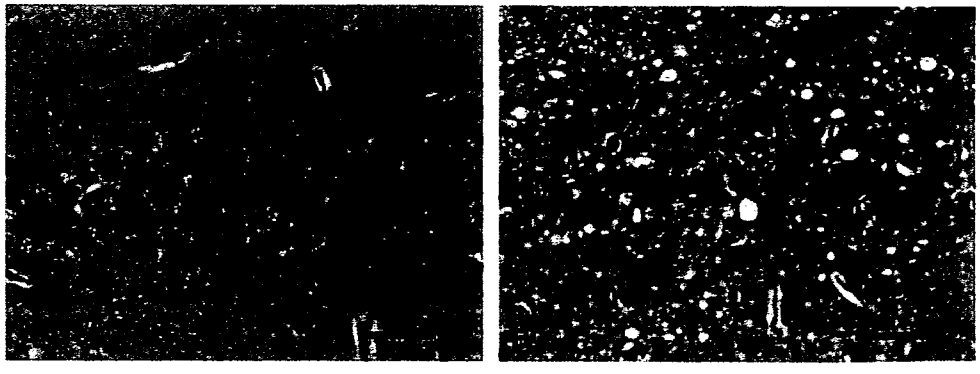

Fig. 3. Typical nerve lesions in the hippocampus of a hamster brain, taken from an animal inoculated with a P-15N-filtered sample (B), in comparison with the corresponding region from an uninfected animal (A). Arrows, vacuolation; Arrowheads, degeneration of nerve cells; scale bar = 50 μm; HE staining used.

"Super-sonication" has the advantage that it is a physical disruption process, and does not alter the chemical composition of the spike material, thus minimizing changes to the start material used for nanofiltration. SD treatment is included in many manufacturing processes for plasma-derived products, and therefore, although not as effective as "super-sonication", use of this treatment might be expected to result in a spike material more closely mimicking the form of infectious prion present in the relevant start material during the manufacturing process. Use of these treatments alone or in combination may therefore be useful in reducing the size of infectious particles present in TSE spike materials for prion clearance studies.

The effect of the above treatments was studied using normal MF, as the facility was unable to handle infectious TSE materials. Although some care should be taken in extrapolating these results to TSE-infected brain material, "super-sonication" of 263K MF preparations appeared to reduce the removal of PrP^{Sc} following filtration, while detergent-treated spike preparations have previously been shown to present a more significant challenge to nanofiltration steps than untreated preparations ([9,10] and own unpublished observations). Furthermore, "super-sonication", with or without SD treatment, does not appear to reduce the level of infectivity present within the 263K MF, supporting the use of such preparations for prion clearance studies.

Using 263K MF treated with 0.1% sarkosyl, "super-sonication" or SD plus "super-sonication", we investigated the prion removal capacity of P-15N, P-20N and P-35N filters in the manufacturing processes used for four different plasma products. The results obtained suggest that both the composition of the materials to be filtered and the prion load influences the removal of prions. PrP^{Sc} was recovered in the filtrate fraction from three out of the four processing steps performed for P-20N and P-35N. In contrast, under all conditions tested, P-15N filtration resulted in removal of PrP^{Sc} to below the limit of detection of the Western blot assays used. Thus, P-15N would appear to be a more robust method for the removal of prions, reproducibly giving LRF in the order of 3 logs, under the conditions tested. In practice, however, it is not feasible to incorporate P-15N filtration into the manufacturing process for all plasma derivatives. From the results shown in Table 2, it may also be possible to optimize processing conditions to allow effective removal of PrP^{Sc} using P-20N or P-35N filters.

WB assays were used to monitor the partitioning of PrP^{Sc} during the nanofiltration processes. WB assays are semi-quantitative and serve to provide an indication of the relative levels of PrP^{Sc} present in different samples. However, there are limitations to the sensitivity of available WB assays, and these assays provide only an indirect measure of infectivity. Therefore, to confirm that removal of PrP^{Sc} does reflect removal of infectivity, bioassays need to be performed.

Although PrP^{Sc} was not detected in any of the P-15N filtered samples by WB assay, infectivity was recovered in a filtrate fraction tested by bioassay for one process run. Foster also noted that infectivity was detected in a filtrate fraction after P-15N filtration ([8] reported as personal communication; data not shown). Thus, even with P-15N, depending on the processing conditions, there may be incomplete removal of prion contaminants.

Although infectivity was detected in the filtrate fraction from the one process step studied, longer and more variable incubation periods were observed in the animals inoculated with the filtrate sample (Table 4), suggesting a lower prion titer following filtration. However, it was not possible to estimate the relative levels of prion infectivity present in the input and filtrate samples, as no data was available to correlate incubation periods and prion titers for this study. Based on the titers typically observed for 263K MF stocks, the bioassay used could theoretically detect reductions in prion infectivity in the order of 4 logs for this process step. Detection of infectivity in the filtrate fraction by bioassay is therefore not necessarily incompatible with the WB results obtained (LRF $\geq$2.8 logs), and may simply reflect a difference in sensitivity between the two assays used.

As discussed above, uncertainties about the nature of the infectious agent in plasma, and during the manufacturing process, raise concerns about the design and interpretation of prion clearance studies. No single spike preparation is likely to contain all potential forms of the infectious agent. Infectivity is associated with membranes and protein aggregates. In addition, it has recently been shown that the GPI anchor is not required for infectivity, suggesting that endogenous proteolytic release of PrP^{Sc} from cell surfaces may also contribute to the spread of the infectious agent *in vivo* [19,20]. Whether significant levels of infectivity in human plasma are associated with GPI-anchorless prion protein is not yet clear. These different forms of infectivity, with different biophysical properties, could show different partitioning properties through the same manufacturing process [7]. Furthermore, different forms of the agent may differ in their level of infectivity. For example, it was recently reported that particles in the order of 17–27 nm appeared to have the highest relative level of infectivity, in comparison to levels of PrP^{Sc} [21]. Therefore, a better understanding of the nature and forms of the infectious agent is essential to allow the design of more accurate models for prion clearance studies, and a more confident evaluation of the safety of manufacturing processes with respect to potential TSE contamination.

In summary, we used methods intended to reduce the size of particles present within MF preparations in an effort to present a worst-case (smallest) prion challenge during nanofiltration. Using such preparations, P-15N filtration consistently reduced the level of PrP^{Sc} to below the limits of detection of the Western blot assays used, suggesting that this process step is effective for the removal of prions. However, data from a single process step studied suggested that infectivity could be recovered following P-15N filtration, and thus even P-15N filtration may not result in complete removal of prions, at least when used under some conditions.

Acknowledgements

A part of this study was presented at the Planova workshop 2003 and 2006 held by Asahi Kasei. Asahi Kasei Medical Co., Ltd. kindly gave us permission to publish the entire study on

Planova filters. Some of the data presented in this study has been summarized in a recent review [22].

References

[1] Health Protection Agency. Fourth case of variant CJD infection associated with blood transfusion. Press release, http://www.hpa.org.uk/hpa/news/articles/press_releases/2007/070118_vCJD.htm, 18 January, 2007.

[2] Castilla J, Saá P, Soto C. Detection of prions in blood. Nature medicine 2005;11(9):982–5.

[3] European Medicines Agency/The Committee for Medicinal Products for Human Use (CHMP)/Biotechnology Working Party. CHMP position statement on Creutzfeldt–Jakob disease and plasma-derived and urine-derived medicinal products. EMEA/CPMP/BWP/2879/02/rev 1. London, http://www.emea.europa.eu/pdfs/human/press/pos/287902rev1.pdf, 23 June, 2004.

[4] The European Agency for the Evaluation of Medicinal Products/The Committee for Medicinal Products for Human Use (CHMP)/Biotechnology Working Party. Guideline on the investigation of manufacturing processes for plasma-derived medicinal products with regard to vCJD risk. CPMP/BWP/5136/03 London, http://www.emea.europa.eu/pdfs/human/bwp/513603en.pdf, 21 October, 2004.

[5] Strengthening of quality and safety assurance of drugs and medical devices manufactured using components of human origin as raw materials. PFSB notification no.0209003 dated February 9, 2005; Japan: MHLW (in Japanese).

[6] Stenland CJ, Lee DC, Brown P, Petteway Jr SR, Rubenstein R. Partitioning of human and sheep forms of the pathogenic prion protein during the purification of therapeutic proteins from human plasma. Transfusion 2002;42(11):1497–500.

[7] Vey M, Baron H, Weimer T, Gröner A. Purity of spiking agent affects partitioning of prions in plasma protein purification. Biologicals 2002; 30(3):187–96.

[8] Foster PR. Removal of TSE agents from blood products. Vox Sang 2004; 87(S2):7–10.

[9] Tateishi J, Kitamoto T, Ishikawa G, Manabe S. Removal of causative agent of Creutzfeldt-Jakob disease (CJD) through membrane filtration method. Membrane 1993;18(6):357–62.

[10] Tateishi J, Kitamoto T, Mohri S, Satoh S, Sato T, Shepherd A, et al. Scrapie removal using Planova® virus removal filters. Biologicals 2001;29(1): 17–25.

[11] Van Holten WR, Autenrieth S, Boose JA, Hsieh WT, Dolan S. Removal of prion challenge from an immune globulin preparation by use of a size-exclusion filter. Transfusion 2002;42(8):999–1004.

[12] Kimberlin RH, Walker CA. Characteristics of a short incubation model of scrapie in the golden hamster. J Gen Virol 1977;34(2):295–304.

[13] Kascsak RJ, Rubenstein R, Merz PA, Tonna-DeMasi M, Fersko R, Carp RI, et al. Mouse polyclonal and monoclonal antibody to scrapie-associated fibril proteins. J Virol 1987;61(12):3688–93.

[14] Lee DC, Stenland CJ, Hartwell RC, Ford EK, Cai K, Miller JLC, et al. Monitoring plasma processing steps with a sensitive Western blot assay for the detection of prion protein. J Virol Methods 2000; 84(1):77–89.

[15] Fraser H, Dickinson AG. The sequential development of the brain lesions of scrapie in three strains of mice. J Comp Pathol 1968;78(3):301–11.

[16] Kärber J. Beitrag zur kollektiven Behandlung pharmakologischer Reihenversuche. Arch Exp Path Pharmak 1931;162:480–3.

[17] Somerville RA, Carp RI. Altered scrapie infectivity estimates by titration and incubation period in the presence of detergents. J Gen Virol 1983; 64(9):2045–50.

[18] Taylor DM, Fernie K. Exposure to autoclaving or sodium hydroxide extends the dose-response curve of the 263K strain of scrapie agent in hamsters. J Gen Virol 1996;77(4):811–3.

[19] Lewis PA, Properzi F, Prodromidou K, Clarke AR, Collinge J, Jackson GS. Removal of the glycosylphosphatidylinositol anchor from PrP^{Sc} by cathepsin D does not reduce prion infectivity. Biochem J 2006; 395:443–8.

[20] Trifilo MJ, Yajima T, Gu Y, Dalton N, Peterson KL, Race RE, et al. Prion-induced amyloid heart disease with high blood infectivity in transgenic mice. Science 2006;313(5783):94–7.

[21] Silveira RJ, Raymond JG, Hughson GA, Race ER, Sim LV, Hayes FS, et al. The most infectious prion protein particles. Nature 2005;437(7056): 257–61.

[22] Yunoki M, Urayama T, Ikuta K. Possible removal of prion agents from blood products during the manufacturing processes. Future Virol 2006; 1(5):659–74.

Available online at www.sciencedirect.com
ScienceDirect
Biochemical and Biophysical Research Communications 362 (2007) 522–524
BBRC
www.elsevier.com/locate/ybbrc

Spectroscopic diagnosis of anti-phospholipid antibodies by visible and near-infrared spectroscopy in SLE patients' plasma samples

Junzo Nojima [a,*], Akikazu Sakudo [b], Yukiko Hakariya [b,c], Hirohiko Kuratsune [c,d], Yasuyoshi Watanabe [e], Yuzuru Kanakura [f], Kazuyoshi Ikuta [b]

[a] *Laboratory for Clinical Investigation, Osaka University Hospital, 2-15 Yamadaoka, Suita, Osaka 565-0871, Japan*
[b] *Department of Virology, Center for Infectious Disease Control, Research Institute for Microbial Diseases, Osaka University, Suita, Osaka, Japan*
[c] *Clinical Center for Fatigue, Osaka City University Medical Hospital, Abeno-ku, Osaka, Japan*
[d] *Department of Health Science, Faculty of Health Science for Welfare, Kansai University of Welfare Science, Kashihara, Osaka, Japan*
[e] *Department of Physiology, Osaka City University Graduate School of Medicine, Abeno-ku, Osaka, Japan*
[f] *Department of Hematology and Oncology, Osaka University Graduate School of Medicine, Suita, Osaka, Japan*

Received 31 July 2007
Available online 13 August 2007

Abstract

The purpose of this study was to investigate whether visible and near-infrared (Vis–NIR) spectroscopy can be used for diagnoses of anti-phospholipid syndrome (APS). Vis–NIR spectra from 90 plasma samples [anti-phospholipid antibodies (aPLs)-positive group, $n = 48$; aPLs-negative group, $n = 42$] were subjected to principal component analysis (PCA) and soft independent modeling of class analogy (SIMCA) to develop multivariate models to discriminate between aPLs-positive and aPLs-negative. Both PCA and SIMCA models were further assessed by the prediction of 84 masked other determinations. The PCA model predicted successful discrimination of the masked samples with respect to aPLs-positive and aPLs-negative. The SIMCA model predicted 42 of 48 (87.5%) aPLs-positive patients and 33 of 36 (91.7%) aPLs-negative patients of Vis–NIR spectra from masked samples correctly. These results suggest that Vis–NIR spectroscopy combined with multivariate analysis could provide a promising tool to objectively diagnose APS.

Keywords: Visible and near-infrared spectroscopy; Anti-phospholipid syndrome; Anti-phospholipid antibodies; Lupus anticoagulant activity; Systemic lupus erythematosus; Enzyme-linked immunosorbent assay

Anti-phospholipid antibodies (aPLs) are a distinct group of autoantibodies that appear in a variety of autoimmune diseases, particularly systemic lupus erythematosus (SLE) [1]. It is now generally accepted that aPLs do not bind primarily to the negatively charged phospholipid itself but rather to complexes of the phospholipid and plasma proteins, and that the most common and well-characterized antigenic targets are β2-glycoprotein I and prothrombin [2,3]. The presence of aPLs is associated with clinical events such as arterial and/or venous thromboembolic complications and obstetric complications [4,5]. Anti-phospholipid syndrome (APS) is diagnosed by both clinical finding (recurrent arterial and/or venous thrombosis and recurrent fetal loss) and laboratory evidence of persistent aPLs [6]. At present, detection of anti-cardiolipin/β2-glycoprotein I antibodies (anti-CL/β2-GPI) and anti-β2-glycoprotein I antibodies (anti-β2-GPI) by enzyme-linked immunosorbent assay (ELISA) and detection of lupus anticoagulant (LA) activity by phospholipid-dependent coagulation assays have been standardized for the diagnosis of APS.

Several clinical studies have established that anti-CL/β2-GPI, anti-β2-GPI and LA activity are present in approximately 40% of patients with SLE and that the presence of these aPLs constitutes a risk factor for arterial and/or venous thrombosis. More recently, some clinical studies

* Corresponding author. Fax: +81 6 6879 6635.
E-mail address: nojima@hp-lab.med.osaka-u.ac.jp (J. Nojima).

0006-291X/$ - see front matter © 2007 Elsevier Inc. All rights reserved.
doi:10.1016/j.bbrc.2007.08.020

indicated that the presence of LA activity detected by a phospholipid-dependent coagulation assay is the strongest risk factor for thromboembolic events in patients with SLE [7]. However, LA activity is heterogeneous with respect to the specificities and functional capacities of the antibodies, and LA activity depends on the ability of autoantibodies to bind to phospholipid-bound β2-GPI or prothrombin [2,3,8]. Therefore, the detection of LA activity requires a careful, sequential series of steps. Despite internationally accepted guidelines and many efforts to improve the standardization of LA assays, it is very difficult to standardize the laboratory diagnosis of LA. Moreover, some investigations showed anti-CL/β2-GPI and anti-phosphatidylserine/prothrombin antibodies (anti-PS/PT) to be independently responsible for the LA activity [9,10]. Therefore, several ELISA methods, including anti-CL/β2-GPI antibodies and anti-PS/PT antibodies are needed for the detection of LA activity. However, these aPLs–ELISA systems are not suitable for the large-scale routine screening that is required for surveillance, because those specific ELISA methods are complicated and high-cost methods. As the first screening examination, the development of an accurate, fast, and low-cost method for the detection of aPLs is needed.

Visible and near-infrared (Vis–NIR) spectroscopy is the spectroscopic method using visible light and NIR radiation [11]. Moreover, Vis–NIR spectroscopy is a fast, multi-component assay that requires no sample preparation and no reagents [11]. Therefore, Vis–NIR spectroscopy has become a widely used analytical method in the agricultural, pharmaceutical, chemical, and petrochemical industries. Recently, Vis–NIR spectroscopy combined with multivariate analysis has been attempted to the diagnosis of viral infection and chronic fatigue syndrome [11,12]. However, it remains unclear whether this analysis method is widely applicable to clinical diagnosis.

In the present study, we examined plasma samples from 118 SLE patients (aPLs-positive group, $n = 64$; aPLs-negative group, $n = 54$) to investigate the ability of Vis–NIR spectroscopy to diagnose the presence of aPLs.

Materials and methods

Samples. We studied plasma samples from 118 patients with SLE (116 females, 6 males; aged 10–75 years, mean 41.7 years). Diagnosis of SLE was made according to the revised criteria of the American Rheumatism Association. Blood samples were taken into vacuum tubes (5.0-ml total volume, SEKISUI, Japan) containing 0.5 ml of 3.13% trisodium citrate ($Na_3C_6H_5O_7{\cdot}2H_2O$), and platelet-poor plasma was prepared by double centrifugation at 2800*g* for 15 min at 15 °C. The plasma samples were frozen at −80 °C until batch assays could be performed. Informed consent was obtained from all patients and control subjects.

Detection of aPLs. The presence of aPLs was detected by 3 different aPLs–ELISA (anti-CL/β2-GPI, anti-β2-GPI, and anti-PS/PT) and LA assay. The concentrations of anti-CL/β2-GPI, anti-β2-GPI, and anti-PS/PT were measured by each specific ELISA system, as described previously [10,13]. LA activity was detected by both the dilute Russell viper venom time (Gradipore Ltd) and STACLOT (Diagnostica Stago) LA tests. The dilute Russell viper venom time and STACLOT LA tests were performed with commercially available screening and confirmatory tests as reported previously [10,13]. We divided 118 SLE patients into two groups (aPLs-positive group, $n = 64$; aPLs-negative group, $n = 54$) according to the APS criteria [6].

Calibration model of PCA and SIMCA. Multivariate analyses such as principal component analysis (PCA) and soft independent modeling of class analogy (SIMCA) are the most useful methods for analyzing Vis–NIR spectra. Plasma samples from 48 aPLs-positive patients and 42 aPLs-negative patients were used as test samples to develop a calibration model of PCA and SIMCA. Moreover, another 48 determinations (16 aPLs-positive patients × 3 spectra) and 36 determinations (12 aPLs-negative patients × 3 spectra) were masked and used for prediction. All samples were diluted 10-fold with phosphate-buffered saline and adjusted to a constant volume (2 ml) in a polystyrene cuvette (SARSTEDT, Aktiengesellschaft, Germany) before Vis–NIR spectroscopy measurement.

Instrument and data collection. Three consecutive Vis–NIR spectra were measured at 2 nm resolution with an NIRGUN (Japan Fantec Research Institute, Shizuoka, Japan) at 37 °C. The spectral data were collected as absorbance values [$\log(1/T)$], where T = transmittance in the wavelength ranged from 600 to 1100 nm.

Data processing. Pirouette software (ver. 3.11; Infometrics, Woodinville, WA) was employed for data processing. To minimize differences between spectra caused by baseline shifts and noise, prior to calibration, spectral data were mean-centered and transformed by standard normal variates (SNV) and smoothing based on the Savitsky–Golay algorithm. To identify the predominant absorbance peaks in the spectra, PCA and SIMCA methods were further applied to develop PCA and SIMCA models for CFS diagnosis, respectively. We used a method of visualizing the SIMCA approach, the Coomans plot, which plots class distances against each other. Coomans plot was applied to assess the classification performance of the SIMCA model by predicting class membership in terms of distance from the model. The critical distance from the model used corresponded to the 0.05 level and defined 95% tolerance intervals. The mathematical formulas used are available in the Pirouette manual.

Results and discussion

Although several specific ELISA methods, including anti-CL/β2-GPI, anti-β2-GPI, and anti-PS/PT, in addition to LA assay are usually used for the detection of aPLs [2,3,9,14], those methods are not ideal in terms of cost effectiveness and speed. We report here the first evidence that the presence of aPLs can be objectively diagnosed by PCA and SIMCA of Vis–NIR spectra of plasma sample.

Vis–NIR spectroscopy is a fast and low-cost method that requires no sample preparation and no reagents [11]. To investigate the ability of Vis–NIR spectroscopy to diagnose aPLs, we examined plasma samples from SLE patients with or without aPLs. Vis–NIR spectra from 90 plasma samples of SLE patients, including 48 in aPLs-positive group and 42 in aPLs-negative group, were PCA and SIMCA to develop multivariate models to discriminate between aPLs-positive and aPLs-negative. Discrimination of the plasma samples of aPLs-positive group from those of aPLs-negative group was seen in PCA scores using first principal component (PC1) and second principal component (PC2). The SIMCA model allowed correct separation of Vis–NIR spectra of 139 of 144 (96.5%) aPLs-negative group and 113 of 126 (89.7%) aPLs-positive group. SIMCA analysis using the Coomans plot demonstrated that plasma classes from aPLs-positive and aPLs-negative did not share multivariate space, providing validation for the

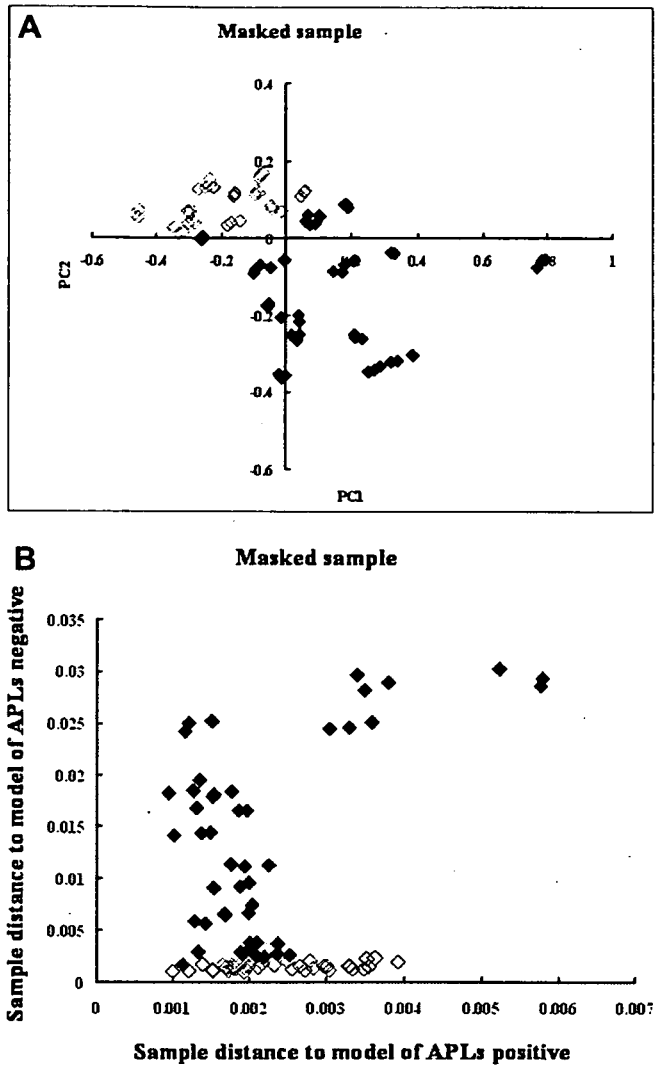

Fig. 1. Spectroscopic diagnosis of anti-phospholipid antibodies (aPLs) by visible and near-infrared (Vis–NIR) spectroscopy. Principal component analysis (PCA) of Vis–NIR calibration and prediction of aPLs diagnosis (A). Soft independent modeling of class analogy (SIMCA) of Vis–NIR calibration and prediction of aPLs diagnosis (B). (◇) aPLs-negative patients. (◆) aPLs-positive patients.

class separation. Both PCA and SIMCA models were further assessed by the prediction of 84 masked other determinations including 48 determinations (16 aPLs-positive group × 3 spectra) and 36 determinations (12 aPLs-negative group × 3 spectra). The PCA model predicted successful discrimination of the masked samples with respect to aPLs-positive and aPLs-negative (Fig. 1A). The SIMCA model predicted 42 of 48 (87.5%) aPLs-positive patients and 33 of 36 (91.7%) aPLs-negative patients of Vis–NIR spectra from masked samples correctly (Fig. 1B).

These findings indicate that Vis–NIR spectroscopy combined with multivariate analysis could provide a promising tool to objectively diagnose the presence of aPLs. Therefore, NIR spectroscopy has great potential as a new method for the diagnosis of APS. This approach deserves further evaluation as a potential novel strategy for instrumental diagnosis of APS. More importantly, NIR spectroscopy can simultaneously measure many components. Further information obtained from detailed analysis of NIR spectra may make significant contributions not only to the diagnosis but also to the understanding of the pathogenesis of APS.

Finally, we would like to emphasize that noninvasive approaches to APS diagnosis are further attractive, because the characteristics of NIR radiation enable nondestructive and non-invasive analysis in vivo. Further studies are currently in progress.

References

[1] G.R. Hughes, The antiphospholipid syndrome: ten years on, Lancet 342 (1993) 341–344.
[2] M. Galli, T. Barbui, Antiprothrombin antibodies: detection and clinical significance in the antiphospholipid syndrome, Blood 93 (1999) 2149–2157.
[3] R.A. Roubey, Autoantibodies to phospholipid-binding plasma proteins: a new view of lupus anticoagulants and other "antiphospholipid" autoantibodies, Blood 84 (1994) 2854–2867.
[4] J.S. Ginsberg, P.S. Wells, P. Brill-Edwards, D. Donovan, K. Moffatt, M. Johnston, P. Stevens, J. Hirsh, Antiphospholipid antibodies and venous thromboembolism, Blood 86 (1995) 3685–3691.
[5] M. Greaves, Antiphospholipid antibodies and thrombosis, Lancet 353 (1999) 1348–1353.
[6] W.A. Wilson, A.E. Gharavi, T. Koike, M.D. Lockshin, D.W. Branch, J.C. Piette, R. Brey, R. Derksen, E.N. Harris, G.R. Hughes, D.A. Triplett, M.A. Khamashta, International consensus statement on preliminary classification criteria for definite antiphospholipid syndrome: report of an international workshop, Arthritis. Rheum. 42 (1999) 1309–1311.
[7] M. Galli, D. Luciani, G. Bertolini, T. Barbui, Lupus anticoagulants are stronger risk factors for thrombosis than anticardiolipin antibodies in the antiphospholipid syndrome: a systematic review of the literature, Blood 101 (2003) 1827–1832.
[8] D.A. Triplett, Lupus anticoagulants/antiphospholipid-protein antibodies: the great imposters, Lupus 5 (1996) 431–435.
[9] T. Atsumi, M. Ieko, M.L. Bertolaccini, K. Ichikawa, A. Tsutsumi, E. Matsuura, T. Koike, Association of autoantibodies against the phosphatidylserine-prothrombin complex with manifestations of the antiphospholipid syndrome and with the presence of lupus anticoagulant, Arthritis. Rheum. 43 (2000) 1982–1993.
[10] J. Nojima, H. Kuratsune, E. Suehisa, T. Kitani, Y. Iwatani, Y. Kanakura, Strong correlation between the prevalence of cerebral infarction and the presence of anti-cardiolipin/β2-glycoprotein I and anti-phosphatidylserine/prothrombin antibodies-Co-existence of these antibodies enhances ADP-induced platelet activation in vitro, Thromb. Haemost. 91 (2004) 967–976.
[11] A. Sakudo, Y. Suganuma, T. Kobayashi, T. Onodera, K. Ikuta, Near-infrared spectroscopy: promising diagnostic tool for viral infections, Biochem. Biophys. Res. Commun. 341 (2006) 279–284.
[12] A. Sakudo, H. Kuratsune, T. Kobayashi, S. Tajima, Y. Watanabe, K. Ikuta, Spectroscopic diagnosis of chronic fatigue syndrome by visible and near-infrared spectroscopy in serum samples, Biochem. Biophys. Res. Commun. 345 (2006) 1513–1516.
[13] J. Nojima, H. Kuratsune, E. Suehisa, Y. Iwatani, Y. Kanakura, Acquired activated protein C resistance associated with IgG antibodies against β2-glycoprotein I and prothrombin as a strong risk factor for venous thromboembolism, Clin. Chem. 51 (2005) 545–552.
[14] J. Nojima, Y. Iwatani, E. Suehisa, H. Kuratsune, Y. Kanakura, The presence of anti-phosphatidylserine/prothrombin antibodies as risk factor for both arterial and venous thrombosis in patients with systemic lupus erythematosus, Haematologica 91 (2006) 699–702.

The Journal of Toxicological Sciences,
Vol.32, No.2, 135-141, 2007

NATIVE STATE OF METALS IN NON-DIGESTED TISSUES BY PARTIAL LEAST SQUARES REGRESSION ANALYSIS OF VISIBLE AND NEAR-INFRARED SPECTRA

Akikazu SAKUDO[1], Etsuro YOSHIMURA[1], Roumiana TSENKOVA[2], Kazuyoshi IKUTA[3] and Takashi ONODERA[1]

[1]*School of Agricultural and Life Sciences, University of Tokyo, Yayoi 1-1, Bunkyo-ku, Tokyo 113-8657, Japan*
[2]*Faculty of Agriculture, Kobe University, Rokkodai 1-1, Nada-ku, Kobe 657-8501, Japan*
[3]*Research Institute for Microbial Diseases, Osaka University, Yamadaoka 3-1, Suita, Osaka 565-0871, Japan*

(Received December 23, 2006; Accepted January 29, 2007)

ABSTRACT — A procedure has been used for the classification and quantification of metals on the basis of a chemometric analysis of visible and near-infrared (Vis-NIR) spectra of metals such as Cu, Mn and Fe in the brain, liver, kidney and testis of mice without digestion. Transmittance spectra in the 600- to 1000-nm region subjected to partial least-squares (PLS) regression analysis and leave-out cross-validation facilitated development of chemometrics models for predicting metal concentration. From the models, Cu, Mn and Fe yielded the coefficients of determination in cross-validation (R^2_{VAL}) as 0.8013, 0.9021 and 0.8295 with standard errors of cross-validation (SECV) of 3.399, 0.8237 and 76.512 μg per g tissue, respectively. The respective detection limits of Cu, Mn and Fe were 12.19, 2.616 and 266.32 μg per g tissue. Furthermore, the regression coefficients of the models showed specific patterns for the respective metals. These results suggest that Vis-NIR spectroscopy may have a great potential for analysis of native state of metals in tissues.

KEY WORDS: Non-destructive, Vis-NIR spectroscopy, Metal, Tissue, Partial least squares regression analysis

INTRODUCTION

Including human beings, living tissues of organisms are composed of only 30 elements (Sharma and Sharma, 1997). Of these elements, 95% represent hydrogen (H), carbon (C), nitrogen (N) and oxygen (O), while the remaining 5% are minerals. Of the minerals, calcium (Ca), phosphorus (P), sulphur (S), potassium (K), sodium (Na), chlorine (Cl), magnesium (Mg), iron (Fe), zinc (Zn), manganese (Mn), copper (Cu), selenium (Se), iodine (I), molybdenum (Mo), chromium (Cr) and cobalt (Co) are essential for normal physiological functions of the living system. Fe, Zn, Mn, Cu, Se, I, Mo, Cr and Co (9 elements) are required in very small quantities and are hence known as "trace elements" (Baran, 2004). A deficiency in or increased exposure to any of these trace elements leads to abnormalities that occasionally may eventuate in pathological conditions (Taylor, 1996). Thus, developments of analytical methods for trace elements are even more important with increasing importance of trace metals recognized for growth and functions of living organisms. Although current methods, such as atomic absorption spectroscopy (AAS) and inductively coupled plasma mass spectrometry (ICP-AES), have been used for detection of trace metals in mammalian tissues (Minami *et al.*, 1995; Verbanac *et al.*, 1997; Morita *et al.*, 1994), these methods are destructive. The main disadvantage of AAS and ICP-AES is a need for a digestion procedure with proper acids.

Visible and near-infrared (Vis-NIR) spectroscopy is a fast multicomponent assay and does not require sample preparations or reagents (Osborne and Fearn, 1986). The NIR and the red regions are dominated by weak overtones and combinations of vibration bands of atoms with strong molecular bonds containing nitro-

Correspondence: Takashi Onodera (E-mail: aonoder@mail.ecc.u-tokyo.ac.jp)

gen, oxygen and/or carbon attached to hydrogen (Osborne *et al.*, 1993). Moreover, as the NIR and red regions have shown relatively weak water absorption with low energy levels, Vis-NIR spectroscopy can be performed without any non-digestive procedures (Ciurczak and Drennen, 2002). It is therefore not surprising that Vis-NIR spectroscopy is an extensively employed analytical method in the agricultural, pharmaceutical, chemical, petrochemical and medical fields (Osborne and Fearn, 1986; Osborne *et al.*, 1993; Ciurczak and Drennen, 2002; Raghavachari, 2001; Sakudo *et al.*, 2005; Sakudo *et al.*, 2006a)

The present study investigated the vibration mode of native states of metals in tissues using Vis-NIR spectroscopy. Hitherto, Vis-NIR spectroscopy has been routinely employed for vibration mode of metals in wines (Sauvage *et al.*, 2002), legumes (Cozzolino and Moron, 2004), forages (Clark *et al.*, 1987, 1989), soils (Moron and Cozzolino, 2003), sediments (Malley, 1998; Malley and Williams, 1997), grasses and hays (Saiga *et al.*, 1989; Smith *et al.*, 1991), where metals are incorporated in complex organic matrices. Although detectable, metals per se exhibit no absorption in the NIR and red regions, since they form complexes with organic molecules containing the C-H, N-H and O-H bonds (Osborne and Fearn, 1986) and water (Sakudo *et al.*, 2006b) that modulate their vibrational modes. Alteration of the vibrational mode has been exploited for distinct metal detection in said agricultural materials (Sauvage *et al.*, 2002; Cozzolino and Moron, 2004; Clark *et al.*, 1987, 1989; Saiga *et al.*, 1989; Smith *et al.*, 1991). In this study, Vis-NIR spectroscopy was used to determine native states of metals in tissues espousing organic matrices by comparing vibration mode using partial least squares regression analysis.

MATERIALS AND METHODS

Animals

Ten male C57BL/6CrSlc mice (Japan SLC, Hamamatsu, Japan) were analyzed at 10 weeks of age. All mice were housed according to standard animal care protocols and sacrificed according to guidelines of the University of Tokyo before harvesting the tissues. Portions of harvested tissues were stocked in a freezer at −80°C before spectroscopic measurements.

Vis-NIR instruments

The frozen tissue samples were thawed and left standing at 25°C to establish a stable temperature. Transmittance spectra of the tissue samples in a cuvette with a polystyrene cell (optical length: 10 mm) (SARSTEDT, Numbrecht, Germany) were measured at 1-nm resolution with a Fruits-Tester-20 spectrophotometer (Japan Fantec Research Institute, Shizuoka, Japan) in an air-conditioned room at 25°C (Fig. 1). Spectral data were collected to yield absorbance value [log (1/*T*)], where *T*= transmittance was measured within the wavelength range of 600 - 1000 nm. Three consecutive spectra were taken from each sample. After collection of Vis-NIR spectra, tissue samples were applied to ICP-AES.

Data processing

Pirouette software (ver. 3.11; Infometrics, Woodinville, WA) was employed for data-processing. To minimize differences between spectra caused by baseline shifts and noise prior to calibration, spectral data were mean-centered and transformed by smoothing based on the Savitsky-Golay algorithm (Savitzky and Golay, 1964). The mathematical formulas are available in the Pirouette manual. The partial least-squares regression (PLS) method was applied to develop the PLS regression model for predicting metal concentrations. The number of PLS factors was chosen from the minimized standard error of cross-validation (SECV). Calculations were performed by leave-out cross validation using 3 spectra after training other samples. The accuracy of the model was evaluated using SECV, while the standard deviation (SD) divided by SECV and the coefficient of determination in cross-validation (R^2_{VAL}) were determined accordingly.

Calculating the detection limits

According to Miller's study (Miller and Miller, 2000), Equation (1) defines the detection limit (y) that indicates if a sample contained a certain metal(s) based on the average (y_B) and standard deviation (S_B) of the signal from the blank control (signal of hypothetical tissues without metals), where the calculated intercept is used as an estimate of y_B Equation (2), which is used to estimate S_B, or statistics $S_{y/x}$, which estimates random errors in the y-direction (Miller and Miller, 2000) The y_i values are the points corresponding to the individual x-values on the calculated regression line:

$$y = y_B + 3S_B \qquad (1)$$

$$S_{y/x} = \left\{ \frac{\sum_i (y_i - \hat{y}_i)^2}{n-2} \right\}^{1/2} \qquad (2)$$

ICP-AES

To minimize metal contamination of samples, all vessels were immersed in 0.1 M HNO_3 overnight and washed with deionized water. Tissue samples were dried at 105°C for 4 hr in a 10-ml polytetrafluoroethylene beaker to obtain the dry weight. Dry weights of tissue samples were as follows. Brain: 114.2-88.2 mg; Liver: 122.9-89.7 mg; Kidney: 75.9-67.4 mg; Testis: 36.5-27.4 mg. The sample and 0.5 ml of concentrated HNO_3 were heated separately from room temperature to 150°C for over 1 hr and then kept at 150°C for 6 hr to promote vapor-phase digestion with HNO_3 in a 50-ml polytetrafluoroethylene digestion vessel with a stainless steel jacket (Takahashi *et al.*, 2003). After cooling to room temperature, the container was diluted to 2 ml with 0.1 M HNO_3. The concentrations of Cu, Mn, Fe and Zn were determined by ICP-AES. Emission intensities were measured using an ICP-AES spectrometer (SPS1200 VR; Seiko, Tokyo, Japan). The respective emission lines used for Cu, Mn, Fe and Zn were 324.754, 257.610, 259.940, and 213.856 nm, and Ar plasma was maintained with an incident power of 1.3 kW.

RESULTS AND DISCUSSION

The Cu, Mn, Fe and Zn concentrations in the brain, liver, kidney and testis of mice were measured by Vis-NIR spectroscopy, while those in tissues were determined by ICP-AES. The transmittance spectra were collected within the wavelength range of 600- to 1000-nm region for constructing PLS models for Cu, Mn, Fe and Zn concentrations. To determine predominant changes in the spectra, two pre-processing were performed; viz., mean-centering of spectra and smoothening of spectra. Mean-centering emphasized the subtle variations in the spectra due to changing species concentrations, while smoothing of all spectra was performed to minimize noise variations. Following the determination of predominant species in the spectra, PLS analysis of pre-processed data was performed. The full cross-validation was then applied to construct the PLS calibration models. SECV of Cu, Mn and Fe reach the minimum values with respective factors of 10, 17 and 9. Thus, the optimal numbers of PLS factors for Cu, Mn and Fe concentrations were found to be 10, 17 and 9, respectively (Table 1). Regression plots and regression coefficients of the PLS model for predicting Cu, Mn, and Fe concentration are indicated in Fig. 2.

Good correlation could be obtained between metal values and predicted values based on Vis-NIR spectroscopy (Fig. 2a, c, e), while several tissue samples were predicted as low value when the actual concentration of Fe was high in the tissue in Fig. 2e.

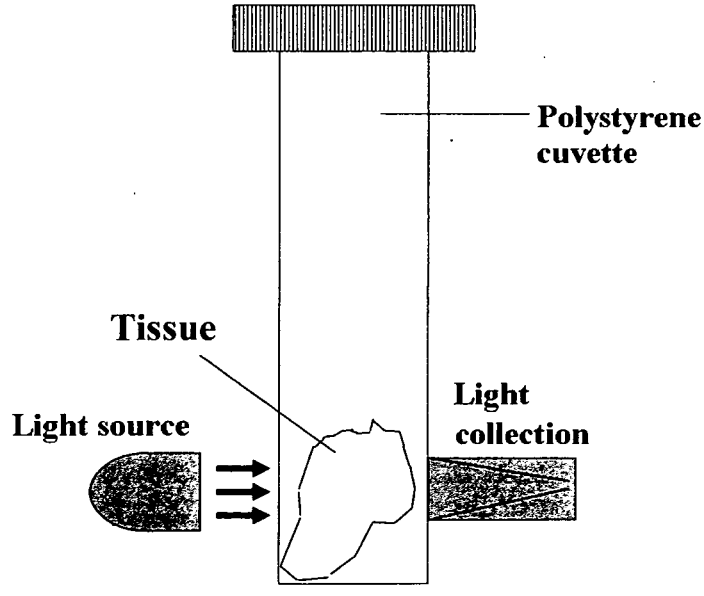

Fig. 1. Schematic representation of non-digestive measurement of a tissue sample by transmittance mode.

Table 1. Statistics of PLS models.

	R^2 VAL	SECV [μg/g dry tissue]	SD/SECV	factors used
Cu	0.8012	3.399	1.62	10
Mn	0.9020	0.8236	2.24	17
Fe	0.8294	76.51	1.74	9

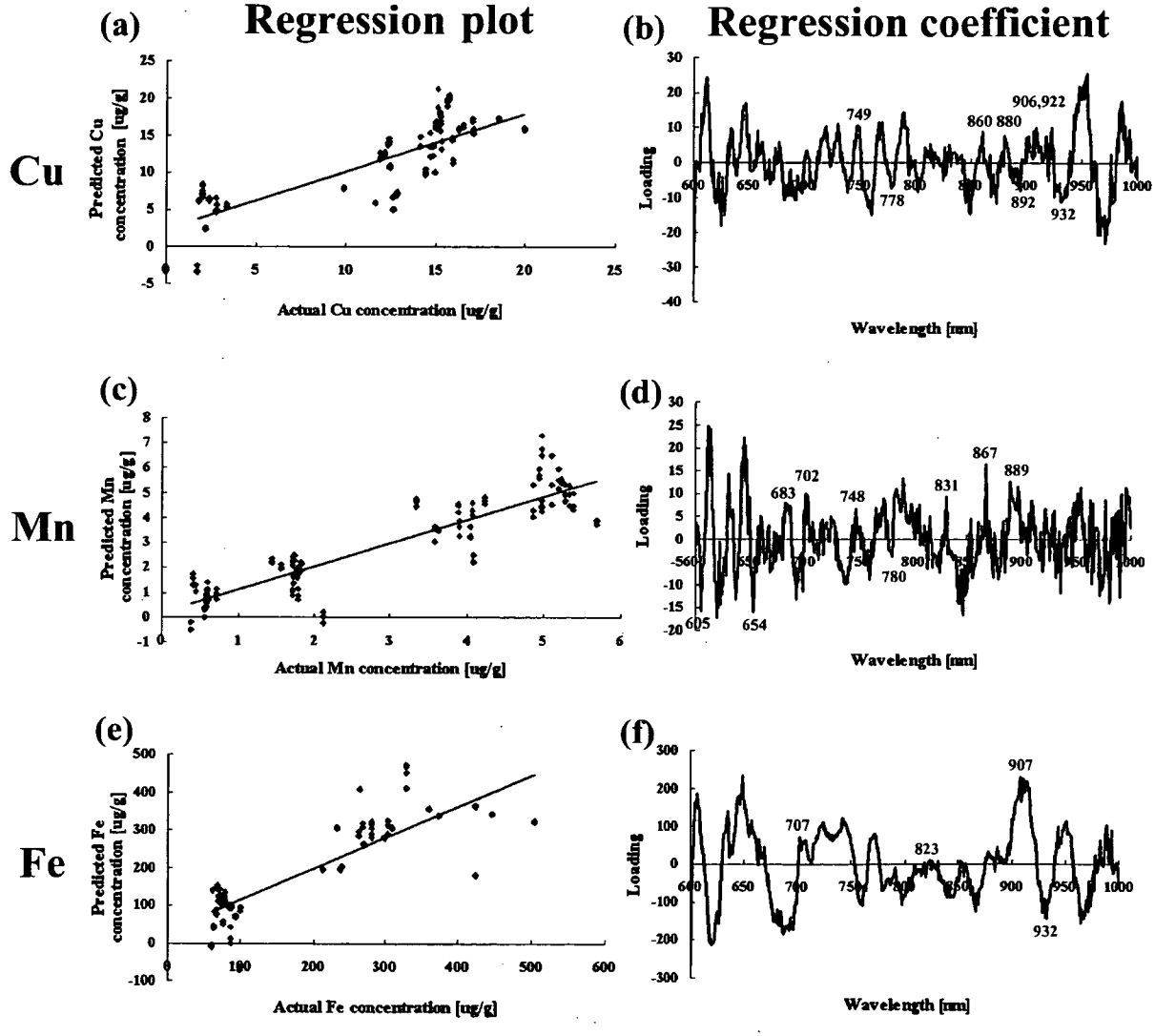

Fig. 2. PLS calibration models for predicting Cu (a), Mn (c) and Fe (e) concentrations in tissues using Vis-NIR spectroscopy.
Cross-validation model: 10 (Cu), 17 (Mn) and 9 (Fe) PLS factors based on a 600- to 1000-nm spectral region using a leave-out cross validation procedure. Loading plots of the regression coefficient for the model based on the Vis-NIR spectra in the 600- to 1000-nm region of Cu (b), Mn (d) and Fe (f) in tissues. Peak wavelengths specific for Cu, Mn and Fe are indicated accordingly.

Although the reason remains unclear, it might be due to light scattering of tissues (Thennadil *et al.*, 2006). Correlation between data and line identity of metals yielded R^2_{VAL} values of 0.801 (Cu), 0.902 (Mn), and 0.829 (Fe). The SECV on the linear regression was calculated to be 3.399 (Cu), 0.8237 (Mn), and 76.51 (Fe) μg per g of dry tissue. The criterion for assessing the models was that R^2_{VAL} >0.70 (Sauvage *et al.*, 2002), although poor when SD/SECV < 1.6; acceptable when 1.6 – 2.0; and excellent implies >2.0 (Moron and Cozzolino, 2003). SD/SECV calculated for metals indicated reliable results; viz., 1.62 for Cu; 2.24 for Mn; and 1.74 for Fe. In contrast, although the development of a PLS calibration model for Zn concentration was also tried, we could not develop an acceptable calibration model to meet the above criteria (data not shown). Therefore, the present study used the wavelength range of 600- to 1000-nm region to generate excellent predictive models for Cu, Mn, and Fe concentrations but not for Zn concentration. Based on Equation (1), the detection limits of the methods for deteremining metal concentrations were thus calculated (Table 2). The respective detection limits of Vis-NIR spectroscopy for Cu, Mn and Fe registered 12.2, 2.6 and 266.3 (Fe) μg/ g dry tissue. As all predicted values of the liver and kidney over the detection limits of Vis-NIR spectroscopy for Cu, Mn and Fe, the PLS model would be applicable to measure Cu, Mn and Fe concentrations in livers and kidneys. However, as other tissues (such as the brain and testis) showed a predicted value below the detection limits for Cu, Mn and Fe, the PLS model might not be applicable. Moreover, Zn is also an important metal found in tissues. Although we endeavored to develop the model for Zn concentration in tissues, we could not develop a model satisfying the criteria.

The PLS modeling provides not only development of quantitative models but also elucidates spectroscopic characterization of samples. Next, to examine spectroscopic characterization of Cu, Mn and Fe in tissues, the regression coefficients for the PLS models were investigated (Fig. 2b, d, f). The regression coefficient contains the model coefficients. A line plot of this object reveals the independent variables (wavelength) important in modeling the dependent variable (metal concentration). Regression coefficients in this model presented peaks corresponding to Cu, Mn and Fe (Table 3). Besides these, many peaks around 610, 620, 630, 640, 690, 720, 740, 760, 770, 790, 800, 850, 870, 950, 970 and 990 nm were commonly observed in the loading of regression coefficients of Cu, Mn and Fe. Although it is often difficult to assign wavelengths to specific molecular absorptions in the NIR and red regions, the commonly observed peaks may be related to interactions between metals and water or organic compounds in tissues such as those of agricultural crops (Sauvage *et al.*, 2002; Cozzolino and Moron, 2004; Clark *et al.*, 1987, 1989; Saiga *et al.*, 1989; Smith *et al.*, 1991). Several peaks for each metal were specifically observed: the peak specific for Cu was detected at 892 nm, while those around 702 and 831 nm (absent for Cu) were indicative of Mn and Fe. Moreover, peaks specific for Mn were also detected at 605, 654 and 683 nm, while those around 910 and 932 nm (absent for Mn) for Cu and Fe were observed as well. No specific peaks for Fe were observed, whereas

Table 2. Detection limits of Cu, Mn and Fe concentrations in tissues by Vis-NIR spectroscopy.

[μg/ g dry tissue]

		Cu	Mn	Fe
Brain	Range (ICP-AES)	9.8 - 14.4	1.4 - 2.1	62.4 - 97.8
Liver	Range (Vis-NIR spectroscopy)	5.0 - 14.6	–0.3 - 2.9	–73.4 - 211.4
	Range (ICP-AES)	14.9 - 19.9	3.3 - 4.2	263.5 - 504.2
	Range (Vis-NIR spectroscopy)	10.0 - 20.0	2.2 - 5.2	140.4 - 363.7
Kidney	Range (ICP-AES)	14.1 - 15.9	4.8 - 5.3	212.2 - 309.7
	Range (Vis-NIR spectroscopy)	11.2 - 21.3	3.4 - 5.3	214.9 - 337.9
Testis	Range (ICP-AES)	1.7 - 3.3	0.3 - 0.7	61.4 - 99.8
	Range (Vis-NIR spectroscopy)	–3.4 - 8.4	–0.2 - 1.8	34.6 - 127.0
Total	Range (ICP-AES)	1.7 - 19.9	0.3 - 5.3	61.4 - 504.2
	Range (Vis-NIR spectroscopy)	–3.4 - 21.3	–0.3 - 5.3	–73.4 - 363.7
	Limit of detection (Vis-NIR spectroscopy)	12.2	2.6	266.3

Tissue samples were digested for ICP-AES and not digested for Vis-NIR spectroscopy.

peaks around 748, 780, 867 and 889 nm (absent for Fe) were representative of Cu and Mn. These results suggest that each metal displayed specific interaction with water or organic functional groups. Several peaks of the regression coefficient were identical to those obtained by other authors using agricultural crops, albeit certain peaks were not commonly shared (Sauvage *et al.*, 2002; Cozzolino and Moron, 2004; Clark *et al.*, 1987, 1989; Saiga *et al.*, 1989; Smith *et al.*, 1991). This is consistent with the notion that the concentration of a metal is measured indirectly by absorbance corresponding to the specific interaction between the metal and water or organic compounds.

The current extensively employed methods for measuring metal concentrations in tissues are AAS, ICP-AES and ICP-MS. It is noteworthy that all these methods are destructive analyses, which require acid digestion. Results in our study suggest that Vis-NIR spectroscopy has the advantage of being a non-digestive analysis for monitoring metal levels in tissues. Furthermore, other advantages of Vis-NIR spectroscopy include prompt analysis, simplicity in sample preparations, and requirements of no chemical reagents. Therefore, Vis-NIR spectroscopy may be used as a large-scale routine assay for measuring metal concentrations in tissues. If Vis-NIR spectroscopy apparatus could be automated, the procedural time would further be abbreviated. Moreover, as the regression coefficients of Cu, Mn and Fe in tissues displayed many distinct peaks, Vis-NIR spectroscopy could therefore discriminate the different metals at native state in tissues.

Table 3. Peaks of regression coefficients for PLS model shown in Fig. 2.

[nm]

Cu	Mn	Fe
	↓605	
↑611	↑614	↑606
↓625	↓620	↓620
↑634	↑631	↑635
↑645	↑645	↑649
	↓654	
	↑683	
↓691	↓693	↓687
	↑702	↑707
↑719, ↑730	↑725	↑724
↓739	↓739	↑742
↑749	↑748	
↓760	↓760	↓758
↑770	↑773	↑771
↓778	↓780	
↑789	↑791	↑791
↓802	↓814	↓800
	↑831	↑823
↓849	↓846	↓846
↑860	↑867	
↓873	↓879	↓866
↑880	↑889	
↓892		
↑906, ↑922		↑907
↓932		↓932
↑954	↑954	↑951
↓971	↓980	↓964
↑985	↑991	↑988

↑: positive peak
↓: negative peak

REFERENCES

Baran, E.J. (2004): Trace elements supplementation: Recent advances and perspectives. Mini Rev. Med. Chem., **4**, 1-9.

Ciurczak, E.W. and Drennen, J.K. (2002): Pharmaceutical and Medical Applications of Near-Infrared Applications (Practical Spectroscopy). Marcel Dekker Inc., New York.

Clark, D.H., Cary, E.E. and Mayland, H.F. (1987): Mineral analysis of forages with near infrared reflectance spectroscopy. Agron. J., **79**, 485-490.

Clark, D.H., Cary, E.E. and Mayland, H.F. (1989): Analysis of trace elements in forages by near infrared reflectance spectroscopy. Agron. J., **81**, 91-95.

Cozzolino, D. and Moron, A. (2004): Exploring the use of near-infrared reflectance spectroscopy (NIRS) to predict trace minerals in legumes. Anim. Feed Sci. Technol., **111**, 161-173.

Malley, D.F. and Williams, P.C. (1997): Use of near-infrared reflectance spectroscopy in prediction of heavy metals in freshwater sediment by their association with organic matter. Environ. Sci. Technol., **31**, 3461-3467.

Malley, D. (1998): Near-infrared spectroscopy as a potential method for routine sediment analysis to improve rapidity and efficiency. Water Sci. Technol., **37**, 181-188.

Miller, J.N. and Miller, J.C. (2000): Statistics and chemometrics for analytical chemistry. Prentice

Hall College Div, UK.

Minami, T., Ichii, M. and Okazaki, Y. (1995): Comparison of three different methods for measurement of tissue platinum level. Biol. Trace Elem. Res., **48**, 37-44.

Morita, A., Kimura, M. and Itokawa, Y. (1994): The effect of aging on the mineral status of female mice. Biol. Trace Elem. Res., **42**, 165-177.

Moron, A. and Cozzolino, D. (2003): Exploring the use of near infrared reflectance spectroscopy to study physical properties and microelements in soils. J Near Infrared Spectrosc., **11**, 145-154.

Osborne, B.G. and Fearn, T. (1986): Near-Infrared Spectroscopy in Food Analysis. Longman Scietific & Technical, UK.

Osborne, B.G., Fearn, T. and Hindle, P.T. (1993): Practical NIR Spectroscopy With Applications in Food and Beverage Analysis (Longman Food Technology). Longman Group United Kingdom, UK.

Raghavachari, R. (2001): Near-Infrared Applications in Biotechnology (Practical Spectroscopy). Marcel Dekker Inc., NewYork.

Saiga, S., Sasaki, T., Nonaka, K. and Takahashi, K. (1989): Prediction of mineral concentration of (Dactylis glomerta L.) orchard grass with near infrared reflectance spectroscopy. J. Jpn. Grass Soc., **35**, 228-233.

Sakudo, A., Tsenkova, R., Onozuka, T., Morita, K., Li, S., Warachit, J., Iwabu, Y., Li, G., Onodera, T. and Ikuta, K. (2005): A novel diagnostic method for human immunodeficiency virus type-1 in plasma by near-infrared spectroscopy. Microbiol. Immunol., **49**, 695-701.

Sakudo, A., Suganuma, Y., Kobayashi, T., Onodera, T. and Ikuta, K. (2006a): Near-infrared spectroscopy: Promising diagnostic tool for viral infections. Biochem Biophys Res Commun., **341**, 279-284.

Sakudo, A., Tsenkova, R., Tei, K., Onozuka, T., Ikuta, K., Yoshimura, E. and Onodera, T. (2006b): Comparison of the vibration mode of metals in HNO_3 by a partial least-squares regression analysis of near-infrared spectra. Biosci. Biotechnol. Biochem., **70**, 1578-1583.

Sauvage, L., Frank, D., Stearne, J. and Millikan, M.B. (2002): Trace metal studies of selected white wines: An alternative approach. Anal. Chim. Acta, **458**, 223-230.

Savitzky, A. and Golay, M.J.E. (1964): Smoothing and differentiation of data by simplified least squares procedures. Anal. Chem., **36**, 1627-1639.

Sharma, R.K. and Sharma, M. (1997): Physiological perspectives of copper. Indian J. Exp. Biol., **35**, 696-713.

Smith, K.F., Willis, S.E. and Flinn, P.C. (1991): Measurement of the magunecium concentration in perennial ryegrass (Lolium perenne) using near infrared reflectance spectroscopy. Aus. J. Agric. Res., **42**, 1399-1404.

Takahashi, M., Terada, Y., Nakai, I., Nakanishi, H., Yoshimura, E., Mori, S. and Nishizawa, N.K. (2003): Role of nicotianamine in the intracellular delivery of metals and plant reproductive development. Plant Cell, **15**, 1263-1280.

Taylor, A. (1996): Detection and monitoring of disorders of essential trace elements. Ann. Clin. Biochem., **33**, 486-510.

Thennadil, S.N., Martens, H. and Kohler, A. (2006): Physics-based multiplicative scatter correction approaches for improving the performance of calibration models. Appl. Spectrosc., **60**, 315-321.

Verbanac, D., Milin, C., Domitrovic, R., Giacometti, J., Pantovic, R. and Ciganj, Z. (1997): Determination of standard zinc values in the intact tissues of mice by ICP spectrometry. Biol. Trace Elem. Res., **57**, 91-96.